Simulation of growth in pyrolytic laser-CVD of microstructures— I. One-dimensional approach

N. Arnold, R. Kullmer and D. Bäuerle

Angewandte Physik, Johannes-Kepler-Universität Linz, A-4040 Linz, Austria

Abstract. Self-consistent model calculations on pyrolytic laser direct writing are presented. The theoretical results are compared with experimental data.

1. Introduction

Pyrolytic laser-induced chemical vapor deposition (LCVD) permits single-step production of microstructures. An overview on the various possibilities of this technique, on the systems investigated, and on the experimental arrangements employed is given in [1].

Elucidation of the microscopic mechanisms involved in pyrolytic laser-CVD and analysis of experimental data require a description of the process on the basis of theoretical approaches. In previous papers we have investigated reaction rates with respect to temperature- and concentration-dependent transport coefficients and with respect to the effects of thermal diffusion and chemical convection [2–4]. Here, we have assumed a purely heterogeneous reaction at the surface of the deposit. The change in the overall reaction flux due to homogeneous gas-phase activation just above the hot surface of the deposit, and due to a backward etching reaction, has been studied in [5]. In all of these calculations, we have ignored the effect of growth on the surface temperature of the deposit. This, however, is a crude approximation, because there is a strong correlation between the geometry of the deposit and the laser-induced temperature distribution. For these reasons, the relation between the laser-induced temperature rise, ΔT, and the absorbed laser-beam intensity is quite complex in general. This problem has been outlined in [1]. Yet, while such types of approaches yield valuable information on the relative contribu-

Correspondence to: Prof. D. Bäuerle, Angewandte Physik, Johannes-Kepler-Universität Linz, A-4040 Linz, Austria.

tion of different mechanisms of gas-phase transport, they do not even permit a semi-quantitative analysis of experimental data.

In this paper we account for this problem and determine the geometry of the deposit from a self-consistent calculation. Here, the equation of growth is solved simultaneously with the laser-induced temperature distribution which, in turn, is approximated by an analytic equation. In this approach, however, we ignore any gas-phase transport and assume a purely heterogeneous reaction. For simplicity, the calculations are performed in *one* dimension. This model can be applied to laser direct writing. The results of these calculations are compared with experimental data on the direct writing of W lines.

2. Model

The model employed in the present calculations is depicted in Fig. 1. Here,

Nikita Arnold was born in 1965, Moscow, Russia. He graduated from Moscow Institute of Physics and Technology in 1987 and obtained his PhD in Physics in 1990. Since 1990 he is a research fellow in the Institute of General Physics, Russian Academy of Sciences, Moscow. In 1991/1992 he was a visiting scientist in the Institute of Applied Physics, Johannes-Kepler-University, Linz, Austria. His research interest is in the field of computer simulations of nonlinear phenomena in distributed systems. He has more than ten publications on this subject.

Roland Kullmer received his diploma in Physics from the University of Kaiserslautern, Germany, in 1982. During his thesis he was concerned with high-resolution laser spectroscopy of SO_2. Since 1985, he is with the Institute of Applied Physics at the Johannes-Kepler-University of Linz, Austria, where he has made contributions in laser-induced chemical processing of materials.

Dieter Bäuerle received his PhD from the University of Stuttgart. Since 1978 he is Professor for Applied Physics at the Johannes-Kepler-University of Linz, Austria. He worked for several years at Cornell University, Ithaca, at the Philips Research Lab in Aachen, and the Max-Planck-Institut for Solid State Research in Stuttgart. He has made contributions in many areas of solid-state physics, laser physics, and spectroscopy, including lattice dynamics, structural phase transitions, high-temperature superconductors, laser chemical processing, and in-situ spectroscopy in reactive systems. He has published over 140 papers, 14 patents, 7 books, and received several awards. He is a member of the Austrian Physical Society, German Physical Society and European Physical Society.
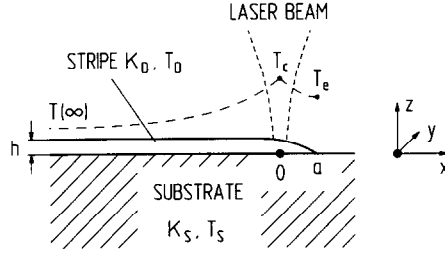
Fig. 1. Schematic for laser direct writing. The coordinate system is fixed with the laser beam. The center of the laser beam of radius w is at the origin $x = 0$; the forward edge of the stripe is at $x = a$. T_c and T_e are the corresponding temperatures. The temperature profile is indicated by the dashed curve. The width of the stripe is $d = 2r_D$.

we consider laser direct writing of a stripe onto a semi-infinite substrate. The respective thermal conductivities and temperatures are denoted by κ_D, T_D and κ_S, T_S. Scanning of the laser beam is performed in the x-direction with velocity v_S. We consider quasi-stationary conditions with the coordinate system fixed with the laser beam. Thus, in this system, the geometry of the stripe remains unchanged; its height behind the laser beam is h, and its width $d = 2r_D$. The temperature distribution induced by the absorbed laser-light intensity is indicated by the dashed curve. Within the center of the laser beam, at $x = 0$, the temperature is denoted by T_c, at the forward edge of the stripe, at $x = a$, by T_e, and with $x \to -\infty$ by $T(\infty)$. The (threshold) temperature at which deposition becomes significant is denoted by T_{th}. Below this temperature the Arrhenius law becomes invalid, as demonstrated experimentally for the case of W deposition [6]. As outlined in [1], changes in the laser-induced temperature distribution, which relate to changes in the geometry of the deposit, are the more pronounced, the more the ratio of thermal conductivities differs from unity. For this reason we consider a case where the ratio of thermal conductivities $\kappa^* = \kappa_D/\kappa_S \gg 1$. This applies, for example, to laser direct writing of thermally well-conducting stripes onto insulating substrates.

2.1. Temperature distribution

The laser-induced temperature distribution is calculated from the energy balance

$$c_D \rho_D F \frac{\partial T_D}{\partial t} = \frac{\partial}{\partial x} \left[F \kappa_D \frac{\partial T_D}{\partial x} \right] - \int_{-r_D}^{r_D} \kappa_S \frac{\partial T_S}{\partial z} \bigg|_{z=0} dy + \mathscr{P}_a = 0. \quad (1)$$

The temperature of the deposit and the substrate is denoted by T_D and T_S, respectively. Here, the influence of scanning has been ignored. This is a good approximation as long as $v_S r_D^2 / [D_S l] \ll 1$. D_S is the thermal diffusivity of the substrate, and l some characteristic length (see below); c_D is the specific heat

and ρ_D the mass density of the deposit. $F \equiv F(x)$ is the cross section of the stripe and $\mathscr{P}_a \equiv \mathscr{P}_a(x)$ the absorbed laser power per unit length. Subsequently, we assume F to be constant, because the heat loss along the stripe is dominated by the region where h and r_D are constant. It can be shown that this approximation is in good agreement with the exact solution of (1) with $F \equiv F(x)$. All parameters, including κ_D and κ_S, have been assumed to be constants. Because $\kappa^* \gg 1$ we have $T_S(z = 0) \approx T_D$. We also approximate the integral in (1) by $\eta \kappa_S \Delta T_D$, where η is a dimensionless geometrical parameter with a value near 2, because $\partial T_S / \partial z \approx \Delta T_D / r_D$, where $\Delta T_D = T_D - T(\infty)$. The radius of the laser beam, w, shall be small compared to r_D so that $\mathscr{P}_a$ can be replaced by $P_a \delta(x) = PA\delta(x)$, where A is the absorptivity. Finally, we introduce the variable

$$l^2 = F\kappa^* / \eta ; \tag{2}$$

l characterizes the drop in laser-induced temperature in the x-direction. With these simplifications and stationary conditions (1) yields

$$l^2 \frac{\partial^2 T_D}{\partial x^2} - [T_D - T(\infty)] + \frac{P_a}{\eta \kappa_S} \delta(x) = 0 . \tag{3}$$

The boundary conditions employed are

$$\left. \frac{\partial T_D}{\partial x} \right|_{x=a} = 0 , \qquad T_D(x = -\infty) = T(\infty) .$$

The solution of this problem for $x < 0$ is:

$$T_D(x) = T(\infty) + \Delta T_c \exp(x/l) , \tag{4}$$

where

$$\Delta T_c \equiv \Delta T(x = 0) = \frac{P_a}{2\eta l \kappa_S} \left(1 + \exp\left[-\frac{2a}{l} \right] \right) ;$$

and for $0 < x < a$:

$$T_D(x) = T(\infty) + \Delta T_e \cosh\left(\frac{x - a}{l} \right) , \tag{5}$$

where

$$\Delta T_e \equiv \Delta T(x = a) = \frac{P_a}{\eta l \kappa_S} \exp\left(-\frac{a}{l} \right) .$$

For the determination of the unknown quantities ΔT_c, ΔT_e, a, F, l, h and r_D, besides (2), (4), and (5) we need four additional equations. The cross section

of the stripe is

$$F \approx \zeta h r_D , \qquad (6)$$

where ζ is a dimensionless geometrical coefficient ($\zeta \approx 2$ for a rectangular stripe, $\zeta \approx 4/3$ for a parabolic cross section, etc.). The width of the stripe is characterized by

$$r_D \approx \xi a , \qquad (7)$$

where ξ is again dimensionless and of the order of unity. It determines the position of the laser beam. The assumption (7) implies that the temperature distribution has axial symmetry near the tip of the stripe and that the threshold temperature, T_{th}, is achieved at the same distance from the center in the x- and y-directions. This is confirmed by both experimental observations and more accurate numerical simulations of the growth process [7]. In other words, the temperature at $x = a$ and $y = r_D$ will be close to the threshold temperature for deposition, i.e.

$$T_{th} \approx \Delta T_e + T(\infty) . \qquad (8)$$

The fourth equation is given by (10).

2.2. Simulation of growth

In a coordinate system that is fixed with the laser beam and with stationary conditions, the height of the stripe is given by

$$\frac{\partial h}{\partial t} = W(T) + v_s \frac{\partial h}{\partial x} = 0 , \qquad (9)$$

where $h = h(x, t)$. $W(T)$ is the growth rate as described by the Arrhenius law, $W(T) = k_0 \exp(-\Delta E^*/T)$, where $k_0 \, [\mu m/s]$ is the pre-exponential factor and $\Delta E^* = \Delta E/k_B$ the apparent chemical activation energy in kelvin. Clearly $\partial h/\partial x \neq 0$ only if $W(T) \neq 0$, i.e. if $T > T_{th}$. If we use for $x = 0$ the approximation $\partial h/\partial x \approx -h/[\gamma a]$, where h is again the (constant) height behind the laser beam, we obtain

$$W(T_c) - v_s \frac{h}{\gamma a} = 0 , \qquad (10)$$

γ is again dimensionless and of the order of unity. Equations (2), (4)–(8), and (10) permit to calculate all relevant dependences. From (3) and (10) we find that with constant v_s the distances r_D, h, a, and l scale linearly with absorbed laser power, P_a. In this case T_c is independent of P_a. The dependence of these quantities on the velocity v_s is more complex. From (4), (5) and (8) we obtain

$$\mu = \frac{a}{l} = \text{arccosh}\left(\frac{\Delta T_c}{\Delta T_{th}}\right), \tag{11}$$

where $\Delta T_{th} = T_{th} - T(\infty)$. From (5) we find

$$l = \frac{P_a}{\eta \kappa_S \, \Delta T_{th}} \exp(-\mu). \tag{12}$$

With (11) this yields

$$r_D = \xi a = \xi l \mu = \frac{\xi P_a}{\eta \kappa_S \, \Delta T_{th}} \mu \exp(-\mu). \tag{13}$$

From (2), (6), and (7)

$$h = \frac{\eta}{\zeta \xi \kappa^*} \frac{a}{\mu^2} = \frac{P_a}{\zeta \xi \kappa_D \, \Delta T_{th}} \mu^{-1} \exp(-\mu). \tag{14}$$

From (10) we obtain

$$v_S = \frac{\gamma \zeta \xi}{\eta} \kappa^* \mu^2 W(T_c). \tag{15}$$

From (11) and (13)–(15) we can calculate h and $d = 2r_D$ as a function of the scanning velocity v_S. Note, that both T_c and μ increase monotonously with v_S.

3. Comparison of theoretical results with experimental data

According to (13) and (14) the width and height of stripes produced by pyrolytic laser direct writing increase linearly with the laser power. This is in agreement with experimental data obtained from many different systems for which the model assumption $\kappa_D/\kappa_S \gg 1$ holds [1].

The dependence of r_D and h on the scanning velocity is more complicated. Figure 2 shows the normalized quantities $h \kappa_D T(\infty)/P_a$ and $r_D \kappa_S T(\infty)/P_a$ as a function of v_S, as calculated from (13)–(15). The respective parameter sets employed are listed in the figure caption. Subsequently, we use only these parameters and geometrical factors. Figure 2 shows that with all parameter sets, the height of the stripes decreases monotonously with increasing v_S. This is quite obvious, because the dwell time of the laser beam decreases with $1/v_S$. The width of stripes, $d = 2r_D$, shows a more complex behavior. In Fig. 2(a) r_D decreases monotonously with increasing scanning velocity, while in Fig. 2(b) it increases monotonously. In Fig. 2(c) r_D first increases up to a maximum value r_D^{max}, which occurs at a velocity v_S^{max}, and then decreases $v_S > v_S^{max}$. The different behavior can be understood from the fact that $r_D(v_S)$ shows a
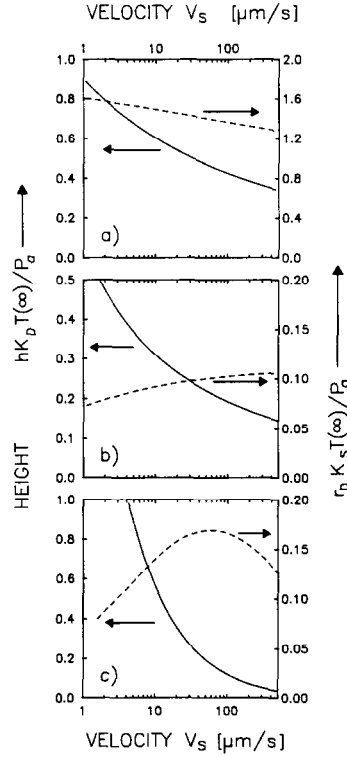
Fig. 2. Normalized width and height of stripes as a function of scanning velocity. The respective parameter sets employed are: (a) $k_0 = 5.3 \times 10^{12}$ μm/s, $\Delta E^* / T(\infty) = 45$, $T_{th}/T(\infty) = 1.17$, $\kappa^* = 30$; (b) $k_0 = 6.6 \times 10^9$ μm/s, $\Delta E^* / T(\infty) = 90$, $T_{th}/T(\infty) = 3.7$, $\kappa^* = 15$; and (c) $k_0 = 16.05$ μm/s, $\Delta E^* / T(\infty) = 5.7$, $T_{th}/T(\infty) = 2.7$, $\kappa^* = 17$. The geometrical factors are the same in all cases: $\eta = 1.6$, $\zeta = 4/3$, $\xi = 1.25$, and $\gamma = 1.3$.

maximum at $\mu = 1$. For this point, we obtain

$$T_c^{max} = T(\infty) + \Delta T_{th} \cosh(1) \approx T(\infty) + 1.5 \, \Delta T_{th} \,,$$

$$r_D^{max} = \xi a = \xi l = \frac{\xi P_a}{\eta \kappa_S \, \Delta T_{th}} \, e^{-1} \,,$$ (13a)

$$h^{max} = \frac{P_a}{\zeta \xi \kappa_D \, \Delta T_{th}} \, e^{-1} \,,$$ (14a)

$$v_S^{max} = \frac{\gamma \zeta \xi}{\eta} \, \kappa^* W(T_c^{max}) \,.$$ (15a)

Thus, the different behavior shown in Fig. 2(a)–(c) is related to the fact that the maximum in r_D can or cannot be observed within a reasonable range of scanning velocities, v_S, depending on the parameter set employed. For materials with *low* deposition threshold (case a) the maximum velocity $v_S^{max} < 1$ μm/s and r_D will thereby decrease monotonously with increasing v_S. For materials

with rather high deposition threshold, r_D may increase monotonously with v_S (case b). Case c represents an intermediate situation. Qualitatively, the occurrence of a maximum in $r_D(v_S)$ is related to the increase in T_c with increasing v_S. This increase in T_c, in turn, is related to the diminished heat flux along the stripe. Let us now compare the behavior of $h(v_S)$ and $r_D(v_S)$ as shown in Fig. 2 with experimental data.

The parameter set employed in the case of Fig. 2(a) refers approximately to pyrolytic laser-CVD of Ni from $Ni(CO)_4$. In fact, experimental investigations on the laser direct writing of Ni lines have shown that r_D decreases with increasing scanning velocity [1, 8].

The parameters employed for calculating the curves presented in Fig. 2(b) describe approximately the deposition of Si from SiH_4 and of C from C_2H_2. For these systems, however, no systematic investigations on the direct writing of lines onto thermally insulating substrates are known.

The parameters employed in Fig. 2(c) are typical for the deposition of W from $WCl_6 + H_2$ [6]. The behavior shown in the figure is, in fact, in qualitative agreement with the experimental results obtained on the direct writing of W lines onto quartz (SiO_2) substrates. For well-defined initiation of the deposition process the substrates were covered with a $h_l \approx 700$ Å thick layer of sputtered W [1]. This layer has been ignored in the calculations which yield a good approximation if $\kappa^* h_l / r_D \ll 1$. In the experiments cw Ar^+-laser radiation ($\lambda = 514.5$ nm; $w \equiv w_0(1/e) = 7.5$ μm) has been employed. Further experimental details are outlined in [1, 6].

Figure 3 shows the height (squares) and width (triangles) of W stripes as a function of scanning velocity for two different partial pressures of WCl_6. The effective incident laser power was the same in both cases. Each data point is an average typically obtained from three different stripes. Full and dashed curves are calculated from (13)–(15) with the same geometrical factors as in Fig. 2. The value of the parameter $\xi = 1.25$ was obtained from experimental data. The other parameters are noted in the figure caption. The height of stripes decreases with increasing velocity v_S. The width of stripes, however, first increases up to a maximum and then decreases with increasing v_S. As expected from (15a), the maximum value occurs at a higher velocity with the higher WCl_6 partial pressure. This is a consequence of the pre-exponential factor, k_0, in the reaction rate $W(T)$. For a partial reaction order of unity with respect to the WCl_6 concentration, k_0 is proportional to $p(WCl_6)$. This describes, at least qualitatively, the trend of the experimental results in Fig. 3. Finally, it should be noted that in pyrolytic laser direct writing instabilities may occur within certain parameter regimes. These result in spontaneous or periodic changes in the width and the height of the stripes [1].

Figure 4 shows the width of W stripes as a function of scanning velocity for different laser powers. The width increases about linearly with laser power; the position of the maximum width, however, remains unchanged. The dashed curves have been calculated by employing the same parameter set as in Fig. 3(a), except of the laser power. With 1.1 mbar WCl_6 and 50 mbar H_2 the results
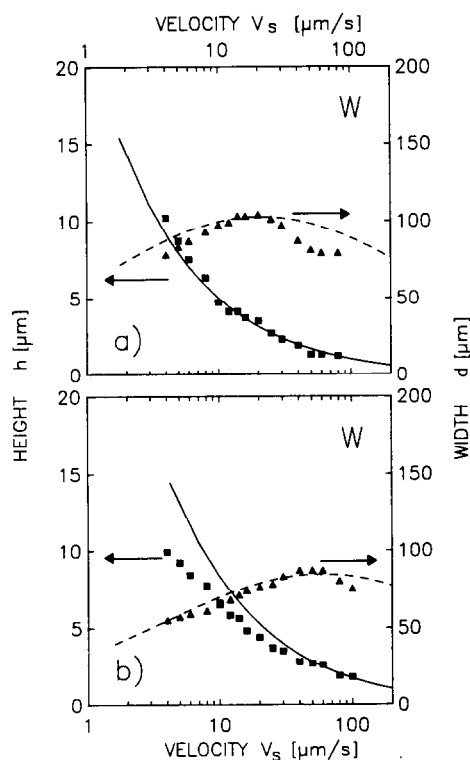
Fig. 3. Width and height of W stripes as a function of scanning velocity for two mixtures of $WCl_6 + H_2$. The H_2 pressure was $p(H_2) = 50$ mbar. The full and dashed curves have been calculated as described in the text. The parameters were $P(514.5$ nm $Ar^+) = 645$ mW, $w_0 = 7.5$ μm, $A = 0.55$, $T(\infty) = 443$ K, $\Delta E^*/T(\infty) = 5.7$, $\kappa^* = 17$, $\kappa_S = 0.032$ W cm^{-1}K^{-1}; $\eta = 1.6$, $\zeta = 4/3$, $\xi = 1.25$, $\gamma = 1.3$. (a) $p(WCl_6) = 0.49$ mbar, $k_0 = 7.15$ μm/s, $T_{th}/T(\infty) = 2.4$; (b) $p(WCl_6) = 1.1$ mbar, $k_0 = 16.05$ μm/s, $T_{th}/T(\infty) = 2.7$.

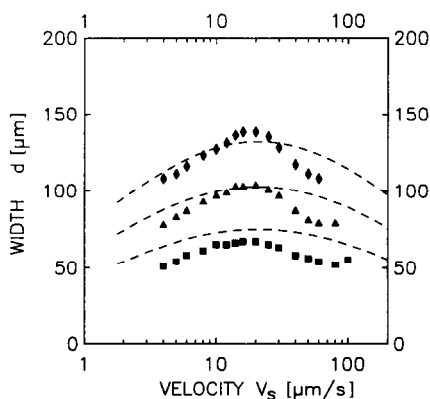Fig. 4. Width of W stripes as a function of scanning velocity for three different laser powers. The precursors employed were 0.49 mbar $WCl_6 + 50$ mbar H_2. The parameters were the same as in Fig. 3(a), except for the laser power; (◆) $P = 825$ mW; (▲) $P = 645$ mW; (■) $P = 475$ mW.
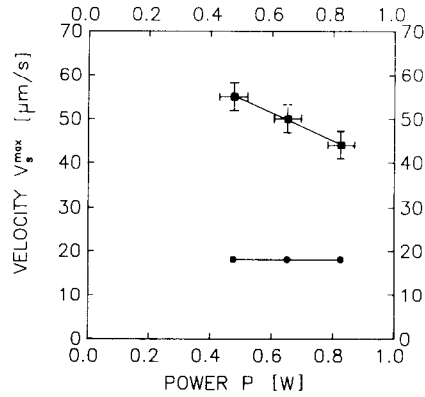
Fig. 5. Scanning velocity v_S^{max} referring to the maximum width of stripes achieved in laser direct writing of W lines from $WCl_6 + H_2$. The partial pressures were $p(H_2) = 50$ mbar and (●) $p(WCl_6) = 0.49$ mbar; (■) $p(WCl_6) = 1.1$ mbar. The other parameters were the same as in Fig. 3.

are similar, except that the maximum is shifted to higher velocities. Figure 5 shows the velocity v_S^{max} corresponding to the maximum width as a function of laser power for $p(WCl_6) = 0.49$ mbar (circles) and 1.1 mbar (squares). The figure shows that v_S^{max} increases by almost a factor of 2.5 when increasing the WCl_6 pressure from 0.49 mbar to 1.1 mbar. This is in qualitative agreement with (15a).

The equations (13a) and (14a) suggest that the maximum height, h^{max}, and width, d^{max}, depend only on the threshold temperature and increase linearly with the laser power. This is also confirmed by the experiments. Figure 6 shows the results for the $WCl_6 + H_2$ system for two different WCl_6 partial pressures. In fact, h^{max} and d^{max} show only a slight dependence on pressure. This can be understood from the small dependence of threshold·temperature on WCl_6 pressure as reported in [6].
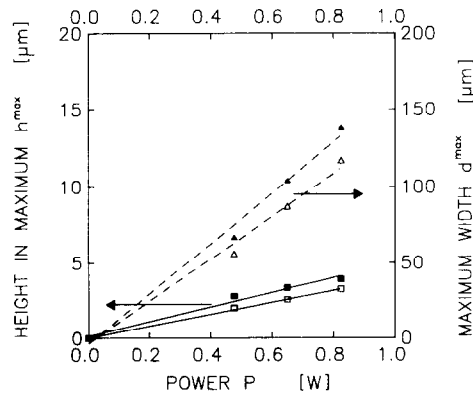

Fig. 6. Maximum width and height of W stripes produced by laser direct writing from $WCl_6 + H_2$. The H_2 pressure was $p(H_2) = 50$ mbar. (■, ▲) $p(WCl_2) = 0.49$ mbar; (□, △) $p(WCl_2) = 1.1$ mbar. The other parameters were the same as in Fig. 3.

Within the approximations made in this model, the agreement between the theoretical predictions and the experimental data must be considered to be quite reasonable. Besides of the simplifying assumptions made, important parameters such as k_0, ΔE^*, and T_{th} can only be estimated from previous experimental investigations. This is true also for reaction orders. The temperature dependences in κ_D, κ_S, and A can be taken into account in a similar approach. Even in this case a linear dependence of r_D, h, a, and l on absorbed laser power is predicted; the maximum center temperature T_c^{max}, will still depend only on T_{th} and the materials' properties. With realistic parameters, the changes in quantities are smaller than 30%.

4. Conclusion

The one-dimensional model presented in this paper permits a semi-quantitative description of many features observed in laser direct writing of thermally well-conducting lines onto insulating substrates.

Acknowledgement

References

[1] D. Bäuerle, Chemical Processing with Lasers, Springer Series in Materials Science, Vol. 1, Springer, Berlin, 1986.
[2] D. Bäuerle, B. Luk'yanchuk and K. Piglmayer, Appl. Phys. A 50 (1990) 385.
[3] N. Kirichenko, K. Piglmayer and D. Bäuerle, Appl. Phys. A 51 (1990) 498.
[4] B. Luk'yanchuk, K. Piglmayer, N. Kirichenko and D. Bäuerle, Physica A 180 (1992) 285.
[5] N. Kirichenko and D. Bäuerle, Thin Solid Films 218 (1992) 1.
[6] R. Kullmer, P. Kargl and D. Bäuerle, Thin Solid Films 218 (1992) 122.
[7] N. Arnold and D. Bäuerle, Microelectron. Eng. 20 (1993) 43.
[8] W. Kräuter, D. Bäuerle and F. Fimberger, Appl. Phys. A 31 (1983) 13.